A Dosimetric Characterization of Novel Formulations of Presage 3D Dosimeters

by

Jacob Lee Jackson

Graduate Program in Medical Physics
Duke University

Date:_____

Approved:

_____
Mark Oldham, Supervisor

_____
Lei Ren

_____
Robert Reiman

Thesis submitted in partial fulfillment of
the requirements for the degree of
Master of Science in the Graduate Program in
Medical Physics in the Graduate School
of Duke University

2014

ABSTRACT

A Dosimetric Characterization of Novel Formulations of Presage 3D Dosimeters

by

Jacob Lee Jackson

Graduate Program in Medical Physics
Duke University

Date:_____

Approved:

_____
Mark Oldham, Supervisor

_____
Lei Ren

_____
Robert Reiman

An abstract of a thesis submitted in partial
fulfillment of the requirements for the degree
of Master of Science in the Graduate Program in
Medical Physics in the Graduate School of
Duke University

2014

Abstract

Purpose: The purpose of this work is to characterize three novel formulations of a radiochromic material Presage and identify optimal imaging procedures for accurate 3D dosimetry. The dosimetric qualities of interest were studied for each formulation of Presage dosimeter in the context of accurate 3D dosimetry. The formulation of Presage showing the most promise is compared to a clinical 3D quality assurance device to investigate the accuracy of a complex state-of-the-art brain IMRT treatment.

Methods and Materials: Three novel formulations of Presage were studied for their temporal stability, sensitivity, linearity of dose response, and feasibility of absolute dose calibration in large volume dosimeters (1 kg) with small volume cuvettes (4g). Large cylindrical dosimeters with 11 cm diameter and 10 cm height were irradiated with 5 2x2 cm fields on the upper flat surface with 3 distinct dose levels (3, 6 and 9.5 Gy, representing low, medium and high). This irradiation pattern is used to determine the dosimetric characteristics mentioned above and was chosen because of its repeatability and it lends to simple measurements of linearity and sensitivity. Measurements were taken at various time points from 0 hours to 24 hours post-irradiation using the high resolution (6.45 μm pixels) Duke Medium-Sized Optical-CT Scanner (DMOS) and reconstructed with a Matlab-based reconstruction GUI created in-house. Analysis of the pertinent dosimetric characteristics was performed in the GUI. A comprehensive end-to-

end QA test was performed on the optimal formulation using optimal scan timing determined from the formulation studies described above. A 5-field IMRT plan was created for head treatment. The plan was delivered both to a head phantom containing a Presage insert, and to the Delta^4 QA device. Comparison of both delivered distributions together with the Eclipse predicted dose distribution enabled investigation of the accuracy of the delivery, and the consistency of independent measurement devices.

Results: The DEA-1 formulation showed up to 10% variation from 0-2 hours post-irradiation, but showed excellent temporal stability (<2% variation) between 3-7 hours post irradiation, and maintained good stability until 24 hours post-irradiation (up to 3% variation). The DEA-2 also showed up to 10% variation from 0-2 hours post-irradiation. The DEA-2 formulation then showed good stability (up to 2.1% variation) from 3-7 hours, but optical density values dropped by up to 11% after 24 hours. The DX formulation did not maintain stability of optical density for any significant time with values decreasing by ~20% by the 24-hour time point and optical density decreasing at different rates for different dose levels. Linearity of dose response was good for all formulations with an R^2 value > 0.99. Gamma analysis with criteria of 3%/2mm was performed on two irradiations of the 5-field pattern on DEA-1 formulation. Voxel passing rates were 96.68% and 97.96%. Comparison of the DEA-1 formulation large dosimeter was done with small volume cuvettes of the same formulation and batch.

Sensitivity of the large dosimeter was less than half the sensitivity of the cuvettes. For clinical 3D QA comparison, the DEA-1 formulation was used because it had optimal performance showed the most promise for accurate 3D dosimetry. Line dose profiles showed that Presage compared very well with the Eclipse calculation and had a much better 3D gamma passing rate for 3%/3mm criteria than the Delta^4 (>99% vs 75%).

Conclusions: The DEA-1 formulation shows the most promise because of its temporal stability and linearity of dose response. The optimal imaging window for this formulation was determined to be 3-24 hours post-irradiation. The DEA-2 and DX formulation also showed potential for accurate dosimetry. The optimal imaging window for the DEA-2 formulation was determined to be 2-6 hours post-irradiation. The optimal scan time for the DX formulation was determined to be immediately post-irradiation. The amount of accuracy loss depending on the scan time is dependent on the formulation and when the dosimeter is scanned. Line dose profiles and gamma analysis results from the comparison of Presage and Eclipse calculation provide strong validation of the accuracy of the IMRT treatment delivery. Comparison of Presage to the Delta^4 show the Delta^4 to be somewhat lacking in its ability to calculate 3D dose in the phantom/Presage geometry.

Contents

List of Tables

List of Figures

Acknowledgements

Mark Oldham, PhD

Titania Juang

John Adamovics, PhD

Lei Ren, PhD

Sarah Ashmeg

1. Introduction

1.1 Advancements in Radiation Therapy Delivery Techniques

Treatment techniques for radiation therapy are constantly improving, and with these improvements come increasing complexity. The past two decades have seen techniques such as intensity-modulated radiation therapy (IMRT), where the multi-leaf collimators (MLC's) move during treatment to better conform dose to the tumor. Volumetric modulated arc therapy (VMAT) is another technique commonly used today in which the MLC's move, the gantry rotates, and the dose rate can be altered during the delivery. Stereotactic body radiation therapy (SBRT) and stereotactic radiosurgery (SRS) are relatively new treatment modalities in which high doses are delivered to precise volumes in few fractions. With these increasing complexities comes the need to verify the complex dose distributions that are being delivered to patients. It is medical physicists' primary responsibility to ensure that the accuracy and precision of more complicated treatment techniques is verified so that the quality of radiation therapy remains high. The Radiological Physics Center (RPC) performed a credentialing study from 2001 to 2011 with their anthropomorphic head and neck phantom in which 763 institutions imaged and delivered an IMRT treatment to the phantom as they would a patient. Of all irradiations in the RPC's database, only 81.6% met the generous acceptance gamma criteria of 7%/4mm [1]. This study demonstrates the need for more strenuous patient-specific quality assurance verification.

1.2 Clinical Quality Assurance

There are two types of quality assurance performed in the clinic: machine QA and patient-specific QA. Machine QA involves daily, monthly, and annual tests of the linear accelerator checking various mechanical and dosimetric characteristics of the machine ensuring that it is delivering radiation accurately and precisely. Patient-specific QA refers to measuring the fluence or dose of the treatment fields of a patient's plan ensuring that it agrees with the calculation provided by the treatment planning system. While the novel dosimeters being discussed in this work may have applications in machine QA, this study will focus on their applications in patient-specific QA

There are several methods of patient-specific QA, including 2D planar measurements, "semi" 3D measurements, and fully 3D measurements. These methods will be discussed further in the following sections.

1.2.1 Two-dimensional Planar Quality Assurance

Two-dimensional planar methods of quality assurance are popular among institutions today. These institutions create a verification plan in the treatment planning system, acquire a CT of the appropriate QA phantom, and then deliver the verification plan to the QA phantom.

Although not as commonly used anymore for patient-specific QA, film dosimetry is a useful tool for 2D quality assurance and is particularly useful for verifying the dose (or fluence) of each beam [2]. Film can be radiographic or

radiochromic in nature. Radiochromic film has several advantages over radiographic film, namely that it requires no developing, is energy independent and approximately tissue-equivalent [3]. Both kinds of film require a calibration curve, which is obtained by irradiating several pieces to a known dose and plotting their optical density against dose. Although easier and more convenient methods of patient-specific QA have been developed, film dosimetry still has an important role in 2D verification of other dosimetric tools.

An increasingly popular alternative to film dosimetry is on-board Electronic Portal Imaging Devices (EPID's). EPID's are a flat panel of amorphous silicon with many small active detector areas and pixel spacing between 0.4 mm and 0.8 mm [4,5]. EPID's are advantageous over film in that they provide faster, digital measurements. There is no inherent build-up region, thus EPID's do not measure dose, but give measurements in "Calibration Units". EPID's can be used to verify the fluence of each treatment field individually, or the treatment fields can be measured compositely with the gantry set to 0^0 for all fields.

Another common planar QA method is done using the MatriXX (IBA Dosimetry), which contains an array of vented parallel-plate ionization chambers. The MatriXX device has 1020 detector elements spaced 7.6 mm apart in a 2D array. Ion-chamber arrays provide a fast and convenient readout, however, they are susceptible to

volume averaging effects, which have to the potential to lead to erroneously high passing rates [6].

MapCHECK is a diode array that is commonly used in patient-specific QA (Sun Nuclear Corp). MapCHECK contains 445 n-type solid-state detectors arranged in a zig-zag pattern with diagonal spacing of 7.17 mm. Diode-arrays also benefit from fast response time and suffer from less volume averaging effect than ion chambers, but have been shown to be dependent on dose-rate and temperature [7].

Two-dimensional planar QA devices are particularly useful for patient-specific quality assurance because they are easy to use. However, with increasingly complex treatment modalities, 2D verification techniques are becoming less adequate in ensuring the accurate treatment of patients. Per beam, planar IMRT quality assurance methods do not accurately predict patient dose errors, and in some cases, high gamma passing rates could lead to significant dose errors in critical structures of the patients' anatomy [8]. This study demonstrates the possible need for more robust and comprehensive dose verification for individual patient treatment plans.

1.2.2 Semi Three-dimensional Quality Assurance

Two of the most prevalent commercially available semi-3D IMRT QA devices used today are the Delta^4 (ScandiDos AB) and the ArcCHECK (Sun Nuclear Corp). Both systems are considered semi-3D because they measure dose at discrete points and

interpolate the dose in between detectors to give an estimated three-dimensional (3D) dose distribution.

The Delta^4 consists of 1069 p-type diodes arranged in a matrix along two orthogonal planes. The diodes have a sensitivity volume area of 0.78 mm^2 and are spaced 5 mm apart in the central 6 cm x 6 cm region. In the outer region, they are space 1 cm apart. The Delta^4 measures the dose for each beam and calculates the dose between diodes by simply using the inverse square law and exponential attenuation. Then, each beam is summed up to obtain the full 3D distribution. Delta^4 has been characterized as an adequate IMRT QA device, however the resulting distribution is not fully 3D [9].

The ArcCHECK is a cylindrical water-equivalent phantom with 1386 diodes arranged in a spiraling geometry along the outer edge of the cylinder. The detectors are spaced 10 mm apart with an active size of 0.8 mm x 0.8 mm. The ArcCHECK has an insert for an ion chamber, which can be used for absolute dose measurement. Similarly to the Delta^4, the ArcCHECK uses interpolation of measurements at discrete points to obtain a 3D dose distribution. Also, it has been shown that the ArcCHECK is limited by field size and angular dependence [10].

Limitations of semi-3D QA devices stem from the fact that they are not fully 3D, and rely on interpolated data to compute 3D dose distribution. Since semi-3D devices are currently used in clinics for verification of complex IMRT and VMAT treatment techniques, a comparison of the performance of a semi-3D device with a fully 3D QA

device could yield valuable insight into the current methods of complex quality assurance.

1.2.3 Fully Three-dimensional Quality Assurance

There are several fully 3D dosimetry techniques, including ferrous sulfate (Fricke) gels, polymer gels, and radiochromic plastic dosimeters.

Fricke gels rely on the dose dependent process of transformation of ferrous ions to ferric ions. Analysis of Fricke gels relies on either optical-CT imaging or MRI measurement of concentration of ferric ions. Fricke gels are convenient in that they can be imaged soon after irradiation; however, their main drawback is ion diffusion with time, which reduces spatial information [11].

Polymer gels are formulated from chemicals that polymerize when exposed to radiation. Polymerization is dose dependent and has the advantage of being able to be read out with MRI, optical-CT, x-ray CT, or ultrasound. Although polymer gels do not exhibit the diffusion limitations of Fricke gels, they are susceptible to atmospheric oxygen inhibiting the polymerization process [12]. In order to hold the gels in place, Fricke gels and polymer gels require a solid container, which is often not tissue equivalent.

Radiochromic plastics consist of a polyurethane matrix doped with a radiosensitive leuco dye. The leuco dye molecules change state from clear to colored (color depends on the type of leuco dye) when irradiated. Radiochromic plastics are

read out with optical-CT, with contrast based on light absorption instead of light scattering. Optical density has been shown to be linearly proportional to dose with little dose-rate dependency [13].

1.3 Presage 3D Dosimetry: Current State of the Art and Limitations

Presage (Heuris Pharma) is a solid polyurethane-based 3D radiochromic dosimeter. The polyurethane is tissue equivalent and contains a free radical initiator and leuco dye, which are responsible for the dose-dependent color change. Adamovics et al. have shown that Presage overcomes some of the limitations of other 3D dosimetry systems such as requiring a container and diffusion of the image [14].

Work by Sakhalkar et al. examined a formulation of dosimeter that exhibited a slight increase in optical density over time [15]. However, the optical density remained linear with dose, and therefore, although the magnitude of optical density increased with time the percent change of optical density with respect to dose remained constant, indicating excellent relative temporal stability. Despite the lack of good absolute temporal stability, it was demonstrated that the Presage/optical-CT has the potential for excellent accuracy, intradosimeter reproducibility, and robustness for use as a 3D relative dosimetry system [14,15].

A study using an advanced multi-target single isocenter VMAT technique showed the feasibility and reproducibility of Presage as a comprehensive 3D QA device [16]. A complex VMAT treatment with 5 arcs delivering dose to 5 separate targets with

doses up to 20 Gy was delivered four times to the head and neck phantom with Presage insert. All four Presage dosimeters were compared to each other using 3%/2mm 3D gamma analysis to assess variation from dosimeter to dosimeter. Results showed consistency (<3% dose deviation) between multiple dosimeters and the treatment plan.

Previous work has shown that the accuracy of Presage is highly dependent on the temporal stability of the dosimeter over time [17]. Varying temporal stability can potentially lead to improper scaling of doses, and therefore, incorrect dose distributions. It was demonstrated with 3D gamma analysis that formulations with better temporal stability had much higher voxel passing rates (98% vs. 85%) than formulations that varied significantly over time.

These prior works have used Presage as a relative 3D dosimetry system. This requires that the optical density measured in Presage be scaled linearly to match the treatment planning system calculation. While relative dosimetry is still useful for quality assurance, an absolute dosimetry system would be more robust for 3D quality assurance applications.

1.4 Goals of this work

The mechanism for optical density change in Presage dosimeters arises from chemical reactions of the leuco dye. This reaction does not complete instantaneously and can be affected by environmental factors such as temperature and room light. For this reason, it is important to characterize how long it takes for all of the chemical reactions

to occur and the optical density of the dosimeter to become stable. Previous formulations have been shown to gradually increase or decrease their optical density with time. While a formulation that clears of color could potentially be useful, the formulations investigated in this study were not investigated for that purpose. Prior formulations have exhibited relative temporal stability, which means that the percent change in optical density with respect to dose is the same for all dose levels, therefore, the relative distribution is "stable" [14]. This study, however, looks to determine a time when novel formulations are absolutely stable. Absolute stability requires that the optical density throughout the dosimeter does not change at all for some amount of time. Absolute stability would enable an accurate calibration of optical density to absolute dose.

The first goal of this work is to investigate several novel formulations of Presage in order to evaluate the post-irradiation reaction kinetics, and to identify the optimal formulations and optimal imaging windows. An ideal formulation would be one that exhibits temporal stability for a reasonable amount of time for optical imaging while also maintaining a linear response with dose. If novel formulations become stable for some amount of time post-irradiation, then the appropriate time to scan the dosimeters can be determined.

A second goal of this work is to investigate the sensitivity of these formulations of Presage as well as the linearity of dose response. Previous formulations have shown

different sensitivities depending on their chemical composition [18]. The sensitivity of the dosimeter defines the maximum allowable dose to be delivered to the dosimeter without risking overexposure, so it is important to understand how sensitive each formulation is to ionizing radiation.

A third goal is to evaluate the accuracy of absolute calibration of dose in large volume dosimeters (1 kg) using small volume cuvettes (4 g). Cuvettes are used to convert the distribution inside the 3D dosimeter from optical density to dose, and its accuracy has been suspect when used to convert dose to a larger volume [19].

The final goal of this work is to evaluate the optimal formulation of Presage/optical-CT against a clinical 3D quality assurance device. Once a formulation with acceptable temporal stability and sensitivity is determined, this formulation will be compared to the Delta^4 for a complex IMRT delivery. The 3D Presage dose distribution will be converted from optical density to absolute dose by inserting an ion chamber into the dosimeter. The overall accuracy of the 3D absolute dosimetry system can then be evaluated compared to the "gold standard" Eclipse treatment planning system. This experiment can also provide validation of the treatment delivery for a complex brain IMRT treatment plan.

2. Methods and Materials

2.1 Presage 3D Dosimeters

Presage is a radiochromic plastic consisting of a liquid polymer which has been mixed with a leuco dye. The leuco dye can be in two chemical states, one that causes it to be clear and one that causes it to be colored. Ionizing radiation causes the change of state of the leuco dye from clear to colored with linear proportion to dose. The melted mixture of polymer and leuco dye is set into a cylindrical shape with dimensions of about 11 cm in diameter and 10 cm tall, which can then be used for 3D dosimetry.

2.1.1 Novel Formulations

The novel formulations to be characterized are called DEA-1, DEA-2, and DX. The chemical components of these formulations that will be reported are the polyurethane matrix, the type and concentration of leuco dye, the type and concentration of leuco dye solvent, and the concentration of initiator. These components are given in the following table for ease of comparison. A brief description of each component and which it was used will be given following the table.

Table 1: Chemical components of three novel Presage formulations

	polyurethane matrix	leuco dye	leuco dye concentration	leuco dye solvent	leuco dye solvent concentration	initiator concentration
DEA-1	SO206	o-MeO-LMG-DEA	1.5%	butyl acetate	5.0%	0.4%
DEA-2	SO206 (40% plasticizer)	o-MeO-LMG-DEA	1.0%	butyl acetate	5.0%	0.4%
DX	SO206	LMG	2.0%	cyclo-hexanone	7.0%	0.75%

The SO206 polyurethane gives a hard clear matrix in which all of the other components are soluble. The o-MeO-LMG-DEA leuco dye used in the DEA-1 and DEA-2 are LMG derivatives and were expected to increase the temporal stability of the dosimeter. The concentration of leuco dye is the primary determining factor of the sensitivity. The butyl acetate dissolves the leuco dye without the need for heating and also increases sensitivity with respect to cyclohexanone. A higher concentration of solvent tends to decrease the temporal stability of the dosimeter. A higher initiator concentration increases sensitivity and Z_{eff}.

2.2 Optical-CT Acquisition

2.2.1 System set-up

The Duke Mid-Sized Optical-CT Scanner (DMOS) was used for acquisition of all data. DMOS was developed in the 3D Dosimetry and Bio-Imaging lab at Duke University. The system is similar to the DLOS (Duke Large field-of view Optical-CT Scanner), which has been previously characterized except it has a smaller field of view

[20,21]. The DMOS system is a bi-telecentric system with <0.1° telecentricity and a magnification of 0.037X. The camera used is a 1040x13921 Basler with a CCD chip. The light source is filtered with a 10 nm bandwidth centered about 633 nm, due to this wavelength having the maximum absorption coefficient for the leuco dye in Presage [22]. The dosimeter is placed in a fluid bath with the refractive index of the fluid matched to the refractive index of the dosimeter. This matching of the refractive indices reduces the bending of the light at the fluid-dosimeter interface. The dosimeter is locked in place by a rotating stage, which allows for projections to be imaged. All dosimeters were imaged with one projection every 1^0 for 360 projections. Each projection was averaged 8 times to eliminate random noise from each projection.

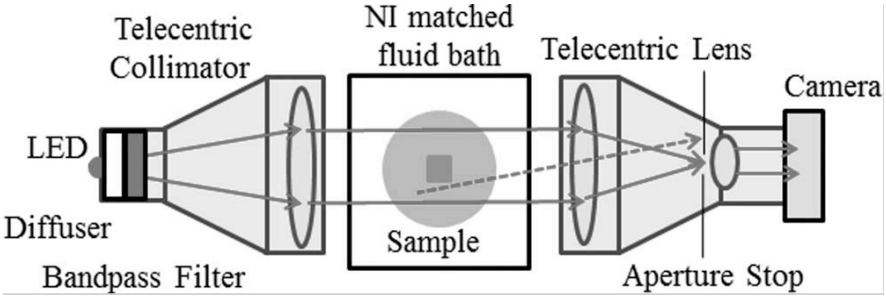

Figure 1: Diagram of bi-telecentric optical-CT system used for Presage readout Image courtesy of Andy Thomas.

2.2.2 Corrections

There are several corrections that must be applied to the images to obtain the highest quality quantitative images. A "dark" correction is applied, which takes care of any imperfections in the CCD. The dark image is acquired by completely covering the

camera lens and capturing 400 averaged images. A "flood" correction is applied to account for any imperfections in the fluid and non-uniformities of the light source. The flood image is acquired by capturing 400 averaged images with only the refractive index matching fluid in the tank.

Because the optical density is the quantity of interest, a pre-scan as well as a post-scan must be acquired, with the flood and dark corrections applied to all projections for both the pre-scan and post-scan.

2.2.3 Timing of post-scans for temporal stability evaluation

The timing of the post-scans is of much importance because of variations of temporal stability for different formulations of Presage. It was desirable to capture the variation in optical density for the first few hours post-irradiation in order to characterize the optimal imaging window for each formulation. Scans were taken immediately post-irradiation, at 30 minutes, at one hour and at every subsequent hour up to 6 hours. One last scan was taken the next day at 24 hours post-irradiation. The dosimeter was not removed from the optical-CT tank between scans for the first 6 hours, however it was stored in the refrigerator over night between the 6-hour scan and the 24-hour scan.

2.3 Optical-CT Reconstruction

All images were reconstructed with a Matlab-based GUI reconstruction program created in the 3D Dosimetry and Bio-Imaging lab at Duke. The reconstruction algorithm

used was filtered backprojection. Images were reconstructed with 2 mm voxel size, using a ramp filter in frequency space. The system has the ability to reconstruct to higher resolution, but 2 mm was chosen to reduce the noise in the images.

2.3.1 GUI conversion of intensity to optical density

Optical density is calculated by taking the logarithm of incident light intensity (counts) divided by the transmitted intensity.

$$OD = \log\left(\frac{I_0}{I_t}\right) \tag{1}$$

Equations 2 and 3 show how the flood and dark corrections are applied to the pre-scan and post-scan. The dark is subtracted from the scan and the flood to account for noise in the CCD. The pre-scan and post-scan are both normalized by their respective flood projections accounting for fluctuating light source output and uniformity.

$$OD = \log\left(\frac{pre-dark}{flood_{pre}-dark}\right) - \log\left(\frac{post-dark}{flood_{post}-dark}\right) \tag{2}$$

$$OD = \log\left(\frac{pre-dark}{post-dark}\right) + \log\left(\frac{flood_{post}-dark}{flood_{pre}-dark}\right) \tag{3}$$

2.4 Five-field Cross Irradiation Pattern

The dosimeter was set up so that the upper flat surface of the cylindrical dosimeter was level with SSD = 100 cm. Each field was 2x2 cm at the surface of the dosimeter. The energy of each beam was 6 MV with a dose rate of 600 MU/min.

The irradiation pattern chosen for evaluating relative temporal stability and the radial variation of sensitivity throughout the dosimeter was a five field cross pattern with three dose levels: 3 Gy, 6 Gy and 9.5 Gy. The monitor units for each beam were calculated so that these dose levels occurred at a depth of 1.5 cm (d_{max}).

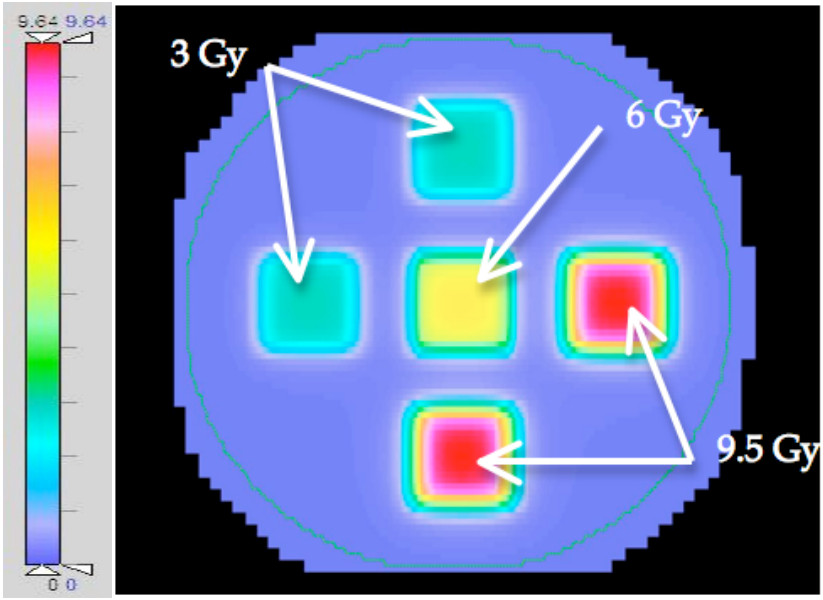

Figure 2: Axial slice at 1.5 cm depth of the dosimeter.

Each field was 2x2 cm and field edges were separated by 1.3 cm. This irradiation pattern was chosen for two reasons. Firstly, it is simple and reproducible for multiple measurements. Secondly, it allows for evaluation of linearity of dose response and sensitivity measurements.

2.5 Eclipse Comparison

After each dosimeter was irradiated and scanned with the optical-CT system, an x-ray CT was taken of the dosimeter on a GE Lightspeed CT scanner. This CT data was

used in the Eclipse treatment planning system to calculate dose inside the dosimeter for the 5-field cross irradiation pattern. The treatment plan was then created in Eclipse to replicate the delivery to the dosimeter.

2.5.1 CERR

CERR (Computation Environment for Radiotherapy Research) is a 3D radiation therapy analysis tool. The Eclipse dose calculation and Presage calculation were imported into CERR for analysis of depth dose profiles and axial dose profiles. Since the monitor units were calculated to deliver the prescription dose to the depth of d_{max}, axial dose profiles were taken in this slice.

2.5.2 Uncertainties of Eclipse

Since the Eclipse treatment planning system is being used as the "gold standard", it is important address any uncertainties associated with it. The field size of all beams delivered in the 5-field cross pattern was 2x2 cm. During commissioning, collimator and phantom scatter factors are only calculated down to field sizes of 4x4 cm, so the $S_{c,p}$ for our delivery had to be interpolated back from larger field sizes. This could lead to a slight error in calculation of monitor units. For the purposes of relative dosimetry, this possible error can be accounted for in the scaling of the Presage readout.

Another possible source of error in the Eclipse calculation occurs in the high-gradient region of the penumbra regions of beams [15, 23]. It's been shown that the accuracy of the modeling of penumbra regions by Eclipse is suspect, and it is likely that

this effect would be more pronounced in small fields such as the ones used in this work. This effect can be attributed to a known dose blurring effect caused by measuring profiles with an ion chamber of finite size (diameter ~6 mm).

2.6 2D independent check

Because of the known dose blurring effect of Eclipse calculations in high-gradient regions, a 2-D independent check of axial line profiles was made with GAFCHROMIC® EBT2 film (ISP corporation, NJ). Two-dimensional film measurements are particularly useful for line dose profiles because of their extremely high resolution and ability for absolute dosimetry.

2.6.1 Film irradiation

The film was placed on top of 8 cm of solid water to provide good scatter conditions. A transparent template of the 5-field cross irradiation pattern was placed on top of the EBT2 film to ensure accurate delivery of the plan. Then, 1.5 cm of solid water was placed on top of the film so that the film was located at d_{max}. The 5-field cross irradiation pattern was then delivered to the film, with each beam having energy of 6 MV and dose rate of 600 MU/min.

2.6.2 Film calibration

In order to convert the measurement of the EBT2 film from optical density to dose, a calibration curve must be acquired. A calibration curve was obtained by cutting several small pieces of film and irradiating them to known doses. The film was placed

between blocks of solid water at a known depth. Each film was then irradiated to a known dose level, with the dose for each film varying between 1 Gy and 10 Gy. One piece of film must also not be irradiated and used as a control. The optical density of each film was then plotted against the known dose of the irradiation.

2.7 Cuvette Calibration

2.7.1 Irradiation of Cuvettes

Cuvettes are small volumes of Presage contained in 1x1x4 cm plastic containers. Cuvettes were irradiated to known doses in order to obtain a calibration curve for converting optical density to absolute dose. Six cuvettes (two cuvettes for each dose level) were irradiated to known dose levels of 3 Gy, 6 Gy, and 9.5 Gy along with two cuvettes as controls that were not irradiated. These cuvettes were placed in solid water at a known depth and surrounded by bolus material to ensure good scatter conditions. Monitor units were then calculated to deliver the appropriate dose to the cuvettes.

2.7.2 Spectrophotometer readout

The cuvettes were scanned before and after irradiation with a spectrophotometer (Genesys 20, ThermoSpectronic) using an empty cuvette to zero the machine. The optical density of the cuvettes of the same dose level was averaged. A linear calibration curve can then be obtained by plotting optical density versus the known dose of the cuvettes for each dose level with the slope being the sensitivity.

2.8 Comparison of optimal Presage formulation to Delta^4 QA device

In order to compare Presage with another QA device, a study was done using both the Delta^4 and Presage. The Presage cylindrical dosimeter was inserted into a head and neck phantom molded from a polyurethane similar to the one used in the dosimeter. Both the head and neck phantom with the Presage insert and the Delta^4 were irradiated with the same treatment plan, and the 3D dose distribution was calculated inside both devices. The case that was chosen for comparison of these two QA devices was a 5-field coplanar brain IMRT plan. This plan was chosen because it is a rigorous test of both devices, and also because the field sizes were all smaller than ~7 cm, so the dose distribution would be contained within the cylindrical Presage dosimeter. Both the Delta^4 and the Presage dosimeter were irradiated with a Varian TrueBeam Stx with high-definition MLCs. The dose distributions were then compared with Eclipse and with each other.

2.8.1 Irradiation technique

During a normal course of radiation therapy, a CT simulation is done first to obtain the necessary CT data for the treatment planning system calculation. In this case, since a CT simulation would contribute a small amount of dose to the Presage dosimeter, a CT simulation was done after irradiation and scanning on the optical-CT system. Although the dose from the CT would have been very small (~1% of the

prescription), it was important in this case to preserve the best technique of Presage/optical-CT readout. Since the irradiation was performed prior to CT simulation, there was no isocenter to align to. The head and neck phantom was aligned using the crosshair in the gantry of the linear accelerator to align to approximately the center of the dosimeter inside the phantom. This isocenter was then marked on the outside of the phantom, and the phantom was irradiated. After the dosimeter was scanned with the optical-CT system, a CT simulation was done. The CT zero was aligned to the isocenter marks on the outside of the phantom, so that the treatment isocenter and the CT zero would coincide at the same point. The treatment plan was then applied to that CT data, and the dose could be calculated inside the phantom.

The Delta^4 was treated with the same brain IMRT plan. The Delta^4 was aligned using the room lasers and external marks to place the isocenter near the center of the diode array where the two planes of detectors meet. The Delta^4 software used the charge recorded in the diodes and ray line tracings through one of the two detectors planes to calculate a 3D dose distribution [9]. The Delta^4 software also has the ability to calculate a 3D dose distribution on the head and neck phantom geometry. It does this by back-calculating energy fluence based on the measurements recorded in the diodes. This back-calculation is done using a pencil-beam algorithm and an iterative optimization process. The software can then be used to forward calculate a dose distribution in the new geometry using the calculated energy fluences.

2.8.2 Analysis in CERR

Analysis of the dose distributions of Presage, Delta^4, and Eclipse was done in CERR. The Presage and Delta^4 distributions were imported into CERR and registered manually to the Eclipse distribution for comparison. Evaluation of all three dose distributions was done using line profiles in axial, sagittal, and coronal planes as well as 3D gamma analysis of Presage vs. Eclipse and Delta4 vs. Eclipse.

2.8.3 Relative vs. Absolute dosimetry in Presage

Presage has primarily been characterized as a relative 3D dosimetry system, however absolute dosimetry is an important next step for Presage [18]. Relative dosimetry was performed in this work by linearly scaling the optical density of the Presage readout to match the Eclipse dose distribution at a point in the high-dose region. Since the dose response is very linear, this is valid and works quite well.

Absolute dosimetry was also performed for the same brain IMRT plan. A cavity for an ion chamber (0.01 cc) was drilled into the bottom of the dosimeter. The head and neck phantom with dosimeter and ion chamber inserted was then irradiated with the same plan that was originally delivered to the phantom. The point dose measured by the ion chamber can then be used to scale the Presage optical density distribution to match the ion chamber reading at that point. The same analysis was performed for both relative dosimetry and absolute dosimetry.

3. Results

3.1 Temporal Stability

The temporal stability of optical density was evaluated using the 5-field cross irradiation of the cylindrical dosimeters. The value of optical density was tracked for each field at a depth of 1.5 cm (d_{max}) for all dosimeters.

3.1.1 DEA-1 stability

The values of optical density have been normalized to the value at the 3-hour time point for each beam to illustrate the variability of each beam in the first 2 hours as well as the excellent absolute stability (<2% variation) of each beam over the next 5 hours. Both 3 Gy beams appear to behave similarly to each other in the first 1-2 hours post irradiation, as do both 9.5 Gy beams. The optical density of both 3 Gy beams increase by ~10% in the first 1-2 hours post-irradiation. The increase in optical density of the 9.5 Gy beams is only ~4% in the first 1-2 hours post-irradiation. The 6 Gy beam along the central axis does not exhibit the same rapid increase in the first 1-2 hours. Four of the five beams also remain stable (~1% variation) for the 24-hour scan, however, the optical density of the beam along the central axis decreases by 3% from the value at 3 hours post-irradiation.

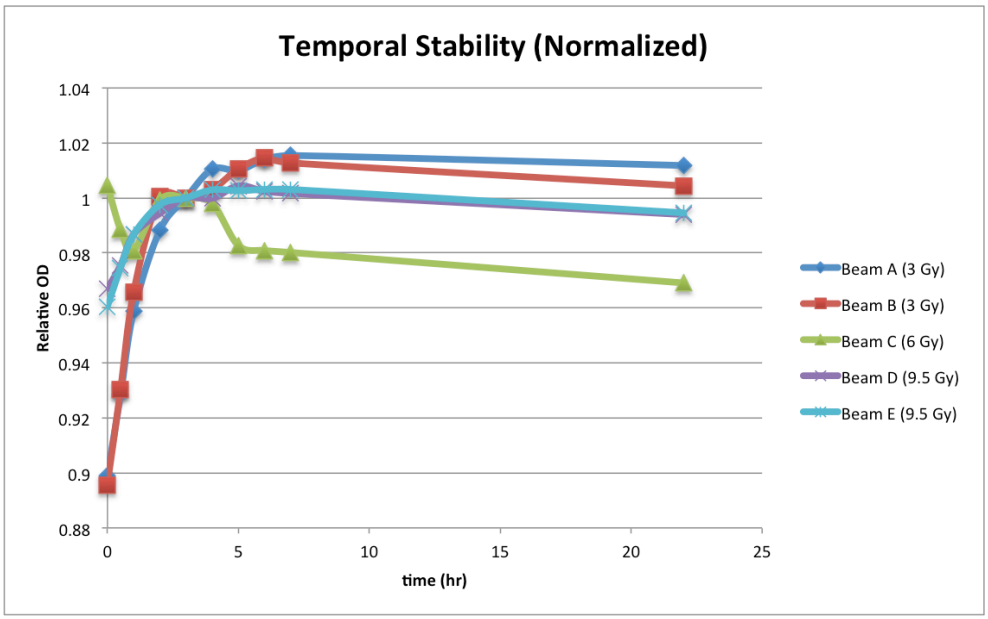

Figure 3: Temporal stability of DEA-1 formulation for large dosimeter.

3.1.2 DEA-2 stability

The values of optical density have been normalized to the value at the 3-hour time point for each beam. There is a rapid change in the first hour, where the values of optical density increase by roughly 4-10%. The optical densities remain somewhat stable (<3% variation) from 3 hours until 7 hours. The optical densities dropped by 3-11% from 7 hours until 24 hours.

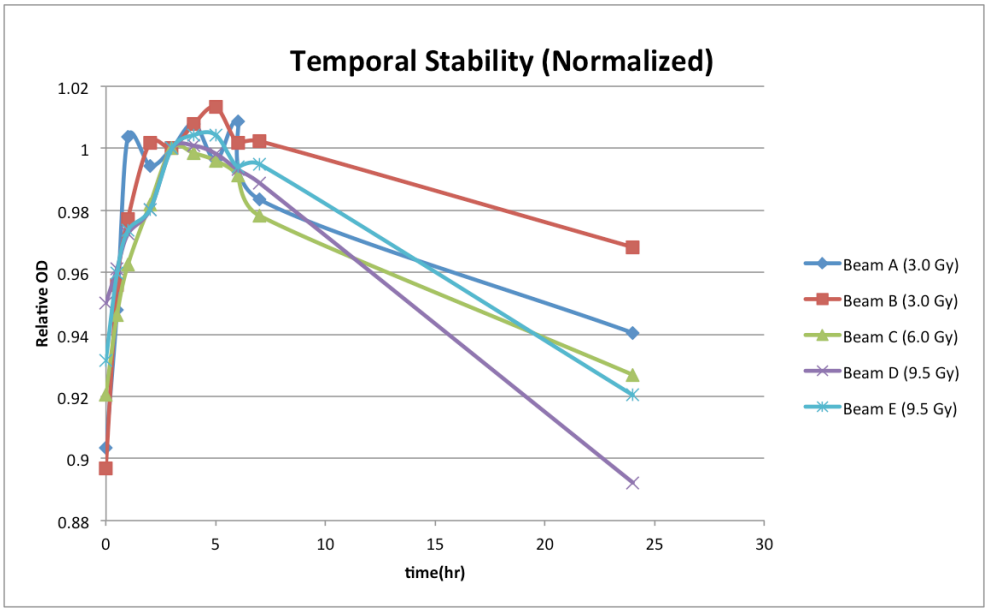

Figure 4: Temporal stability of DEA-2 formulation for large dosimeter.

3.1.3 DX stability

The optical density values have been normalized at 3 hours for each beam for consistency with the other two formulations. There is no rapid change in optical density for any of the 5 beams in the first 1-2 hours post-irradiation. The 3 Gy beams seem to remain stable between 1 and 6 hours post-irradiation with less than 2% variation. The 6 Gy beam remains stable between 0 and 5 hours post-irradiation with less than 2% variation, and after 5 hours the optical density value begins to decrease. The 9.5 Gy beams are never stable for a significant amount of time and decrease continuously from immediately after irradiation until the last measurement was taken at 21 hours.

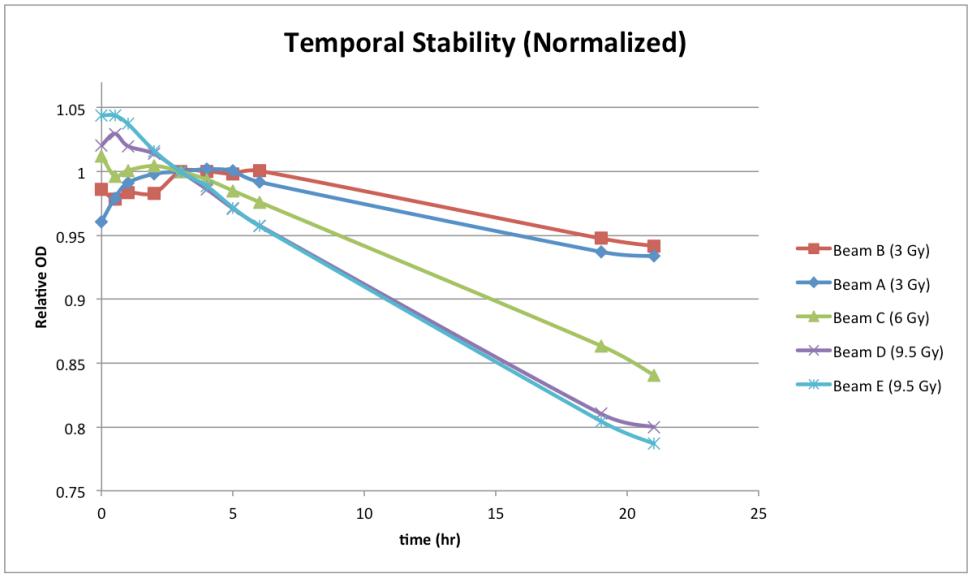

Figure 5: Temporal stability of DX formulation for large dosimeter.

3.2 Sensitivity and linearity of dose response

The sensitivity was measured using the same axial slice (1.5 cm depth) as was used for temporal stability measurements. The optical density values obtained for each beam in that slice were plotted against the dose calculated by the treatment planning system. The following three plots show the sensitivity of each formulation plotted over time. At the 4-hour time point, the DEA-1 formulation shows an average sensitivity of 0.0153 OD/Gy/cm with a variation of ±3.8%. At the 4-hour time point, the DEA-2 formulation shows an average sensitivity of 0.0271 OD/Gy/cm with a variation of ±5.4%. At the 4-hour time point, the DX formulation shows an average sensitivity of 0.0384 OD/Gy/cm with a variation of ±5.9%. However, at the 0-hour time point, this formulation shows an average sensitivity of 0.0387 OD/Gy/cm with a variation of only ±3.2%. Error bars were estimated to account for uncertainties in the optical density

value due to Presage noise (±1%), Eclipse leakage modeling (±0.2%), and set-up errors (±0.0833%). These errors were summed in quadrature to obtain a total error estimate of ±1.02%.

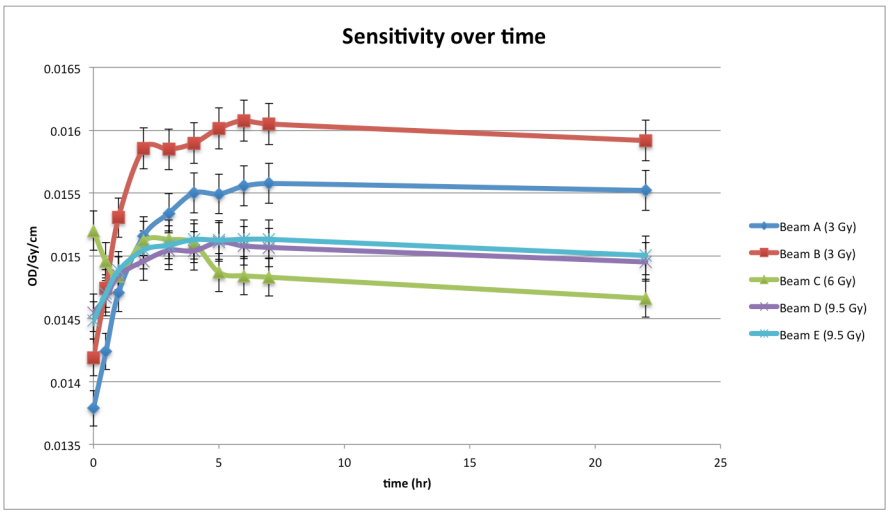

Figure 6: Sensitivity (OD/Gy/cm) of DEA-1 formulation in large dosimeter plotted for each beam over time.

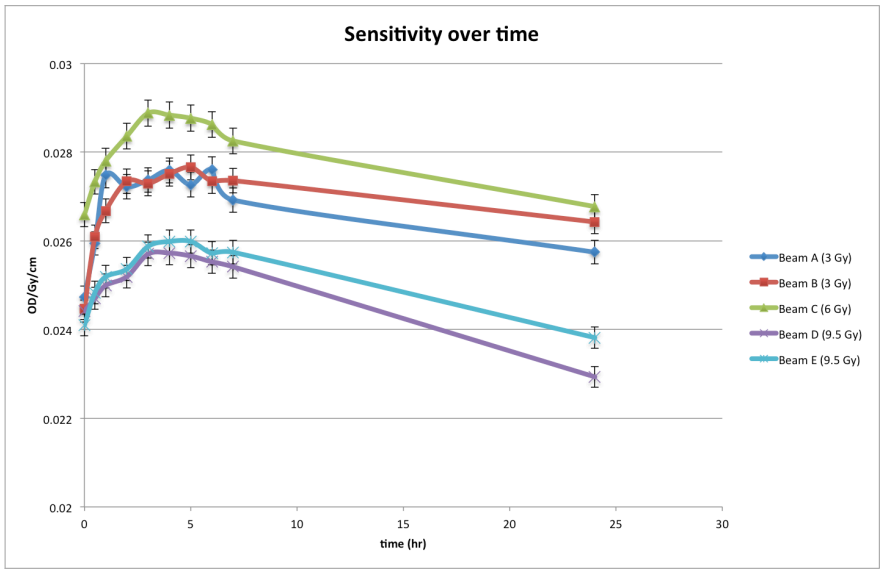

Figure 7: Sensitivity (OD/Gy/cm) of DEA-2 formulation in large dosimeter plotted for each beam over time.

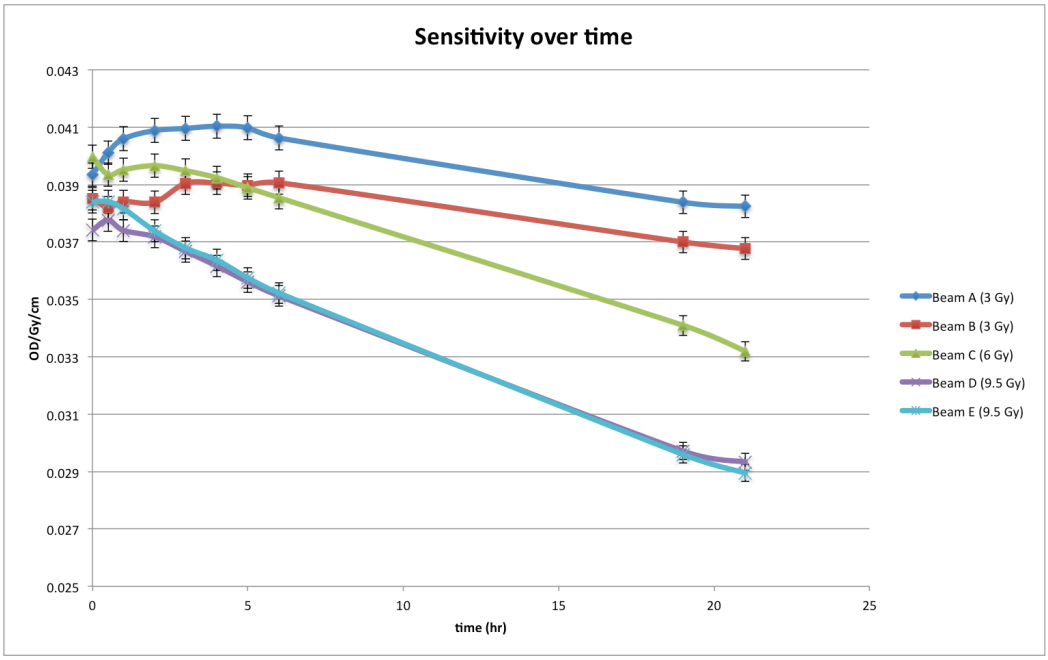

Figure 8: Sensitivity (OD/Gy/cm) of DX formulation in large dosimeter plotted for each beam over time.

The following sensitivity plot shows the sensitivity for all three formulations on the same graph for comparison. It is important to note that the optical density values for all 5 beams are plotted on the sensitivity plots, although the plots may appear to have only 3 points. This is because the values for each 3 Gy or 9.5 Gy beam may be very close to the value of the other 3 Gy or 9.5 Gy beam and will fall right on top of one another.

Using the temporal stability data as a guide, this plot was created using the data from the 4-hour scans of the DEA-1, DEA-2 and DX large dosimeters. The slope of the plot gives the sensitivity. The sensitivity of the DEA-1 formulation is 0.0152 OD/Gy/cm. The linearity of dose response for this formulation is excellent with an R^2 value of

0.99983. It should also be noted that this linear regression has an intercept of 0.0032 OD/Gy/cm. Theoretically, the intercept of the linear regression should be very close to zero, and the cause of this intercept is not known. The consequences and conclusions of this phenomenon will be discussed later. The sensitivity of the DEA-2 formulation is 0.025 OD/Gy/cm with a linearity of $R^2 = 0.99288$. Again, there is a slight positive intercept of 0.0113 OD/Gy/cm. The DX formulation is the most sensitive with a slope of 0.0344 OD/Gy/cm. The linearity of the regression is $R^2 = 0.99737$. This formulation of also exhibits a positive intercept of 0.0201 OD/Gy/cm.

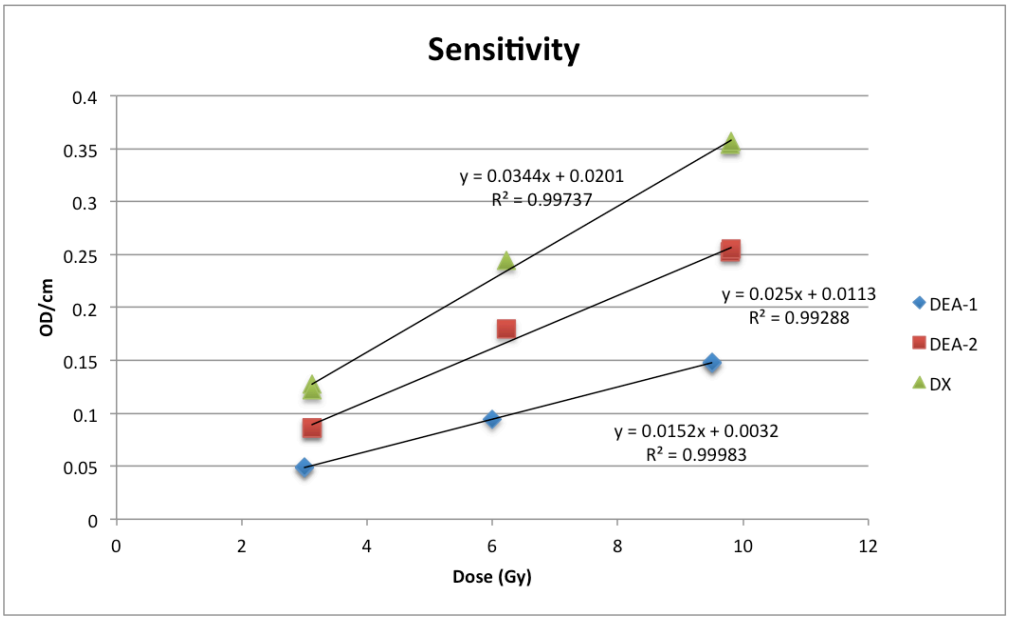

Figure 9: Sensitivity curves plotted for DEA-1, DEA-2, and DX formulations using 4-hour scan and axial slice at 1.5 cm depth. Slope of each curve gives sensitivity of the formulation.

Table 2: Sensitivity, linearity, and intercept of all three novel formulations

	Sensitivity (OD/Gy/cm)	Linearity	Intercept (OD/Gy/cm)
DEA-1	0.0152	0.99983	0.0032
DEA-2	0.025	0.99288	0.0113
DX	0.0344	0.99737	0.0201

3.3 Comparison with Eclipse

Axial, sagittal, and coronal images are shown below with line dose profiles to illustrate image quality, noise, and agreement with Eclipse. There are no noticeable artifacts in this slice of Presage, and the dose profiles show little to no noise. This is due to the reconstruction to 2 mm voxel size of the Presage distribution, which results in some voxel averaging and smoothing of the images. The peak dose of each beam matches well with the Eclipse calculation (<1% difference), however the vertical profile shows the high gradient region to be more rounded off in the Presage distribution than in the Eclipse distribution. This could be due to the high-gradient blurring effect mentioned earlier.

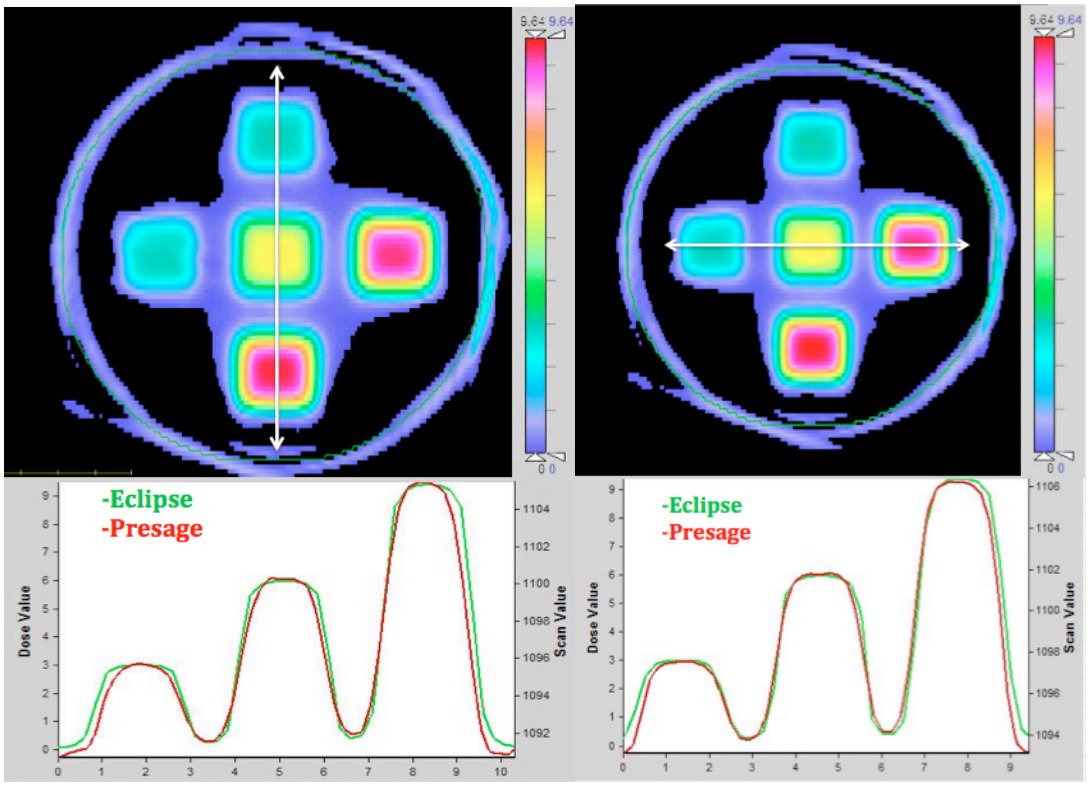

Figure 10: Vertical line dose profile (left) and horizontal line dose profile (right) through axial slice at 1.5 cm depth of Presage measurement in DEA-1 formulation. Profiles show comparison between Presage dose and Eclipse calculation.

Depth dose profiles were also taken for each beam. The plots of depth dose profiles are shown below. The top and bottom slices of the Presage distribution were cropped because of an edge enhancing effect at the top and bottom surfaces of the dosimeter. The depth dose profiles for the 3 Gy beams appear to have the worst agreement with differences between Presage and Eclipse of up to ~9%. The depth dose profile for the 6 Gy beam has disagreement up to ~1.5%, while the depth dose profiles for the 9.5 Gy beams have disagreement up to ~2%.

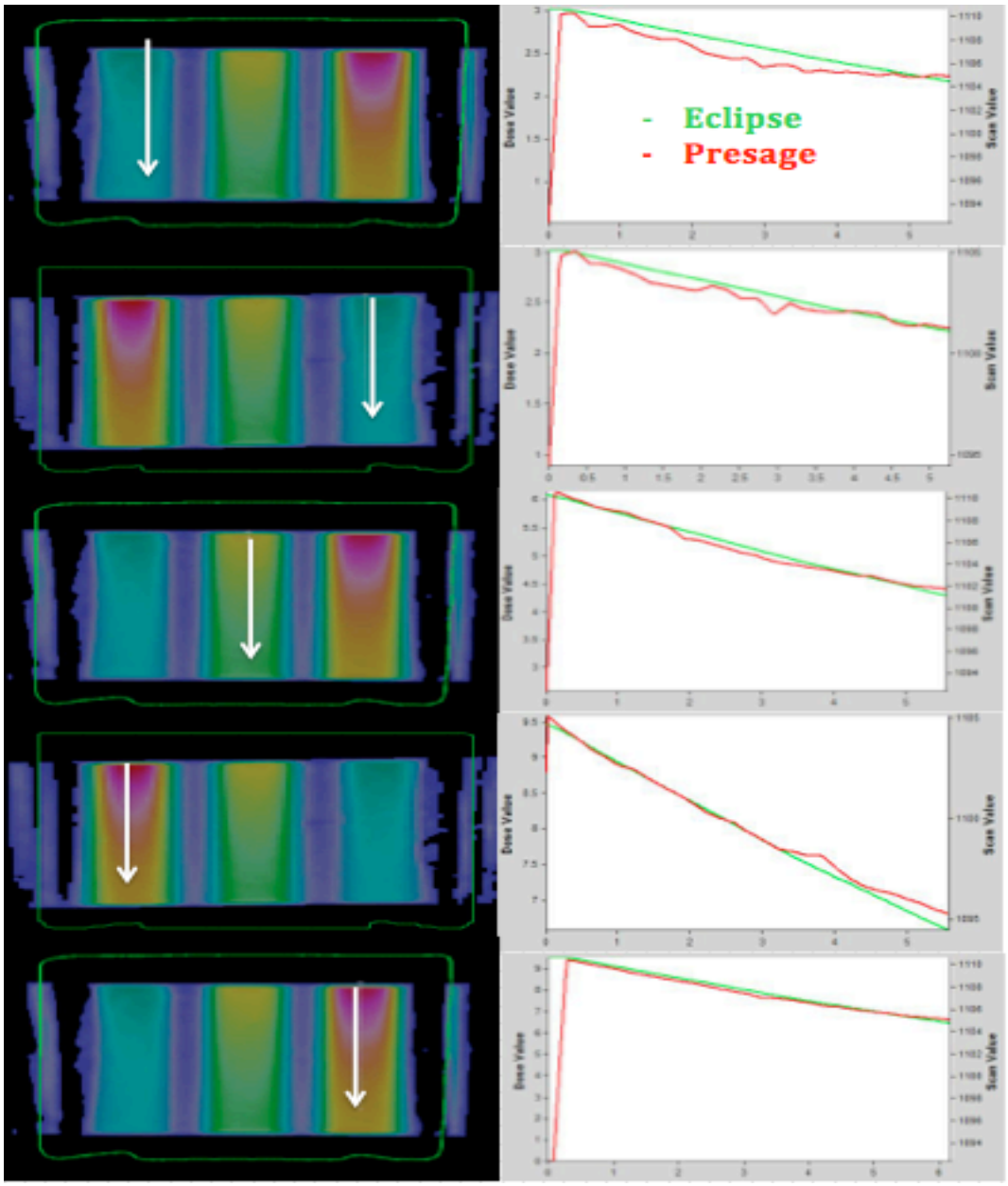

Figure 11: Depth dose profiles for all 5 beams in DEA-1 formulation. Top two profiles are 3 Gy beams, middle profile is 6 Gy beam, and bottom two profiles are 9.5 Gy beams.

The 5-field irradiation pattern was repeated on the DEA-1 formulation. Gamma maps were generated for both irradiations between the Presage dose distribution and Eclipse calculation using a criteria of 3%/3mm. The percentage of voxels passing the gamma analysis (voxels <1.0) for the left dosimeter was 98.2%. The voxel passing rate for the right dosimeter was 99.9%. Most of the regions of failure appear to be in the high-gradient regions.

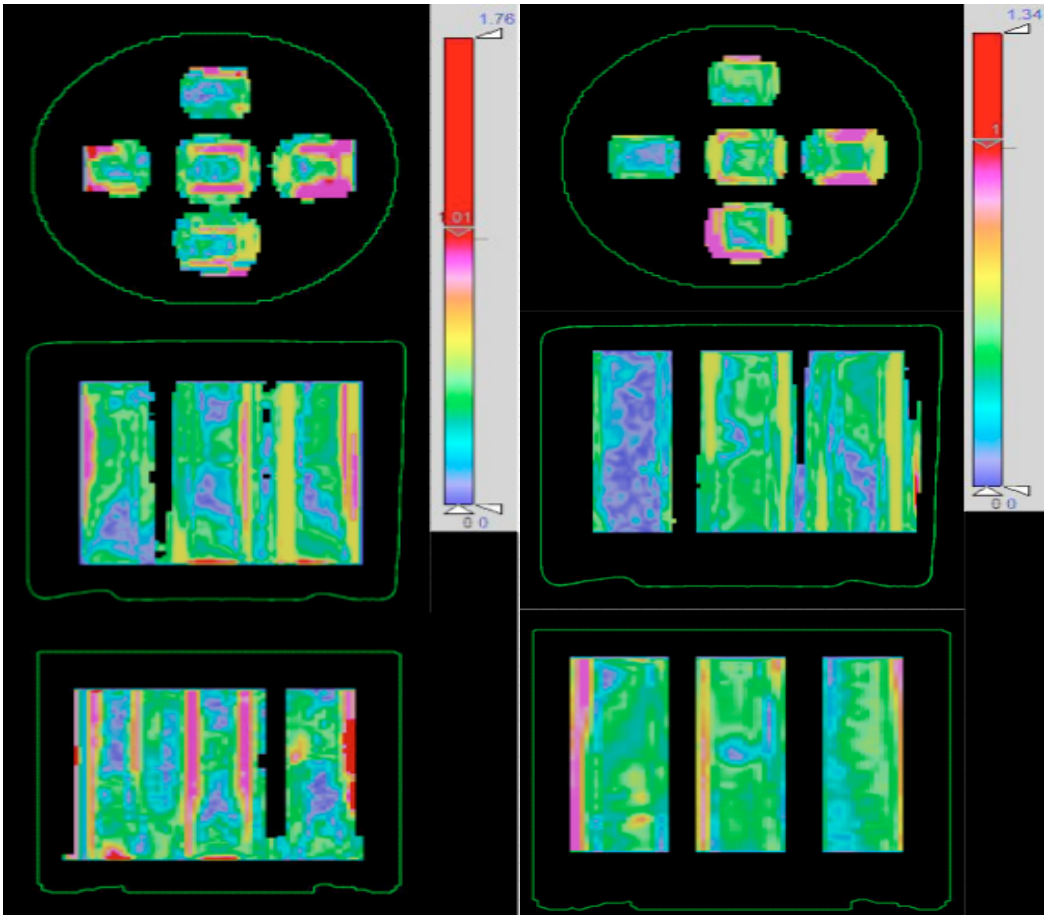

Figure 12: Gamma maps for two irradiations of the 5-field pattern on independent dosimeters of DEA-1 formulation. Criteria of 3%/3mm was used to compare Presage to Eclipse calculation for both dosimeters. Voxel pass rate for left dosimeter was 98.2%. Voxel pass rate for right dosimeter was 99.9%

3.4 Independent 2D film measurement

The 2D film measurement serves to verify the shape of the penumbra of each beam. The general shape of each field appears to be similar in both film and Presage, however there seems to be some slight misalignment issues. Since each treatment field was set up independently for both the Presage and film measurements, this could have lead to some compounding misalignments. The maximum dose at the center of each of the beams showed disagreement of up to 2% for all beams except the 9.64 Gy beam in the horizontal profile. This beam showed disagreement up to ~4%.

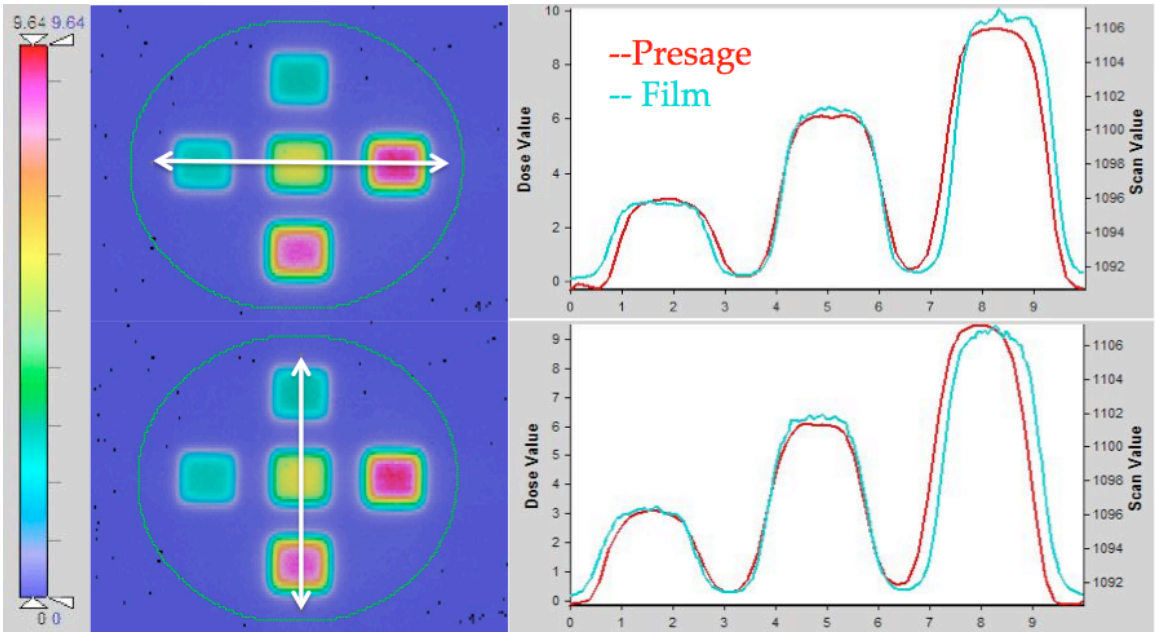

Figure 13: Horizontal (top) and vertical (bottom) dose profiles taken through film and large dosimeter at same slice. General agreement of the shape of each beam is shown, however there appears to be misalignment of some of the beams.

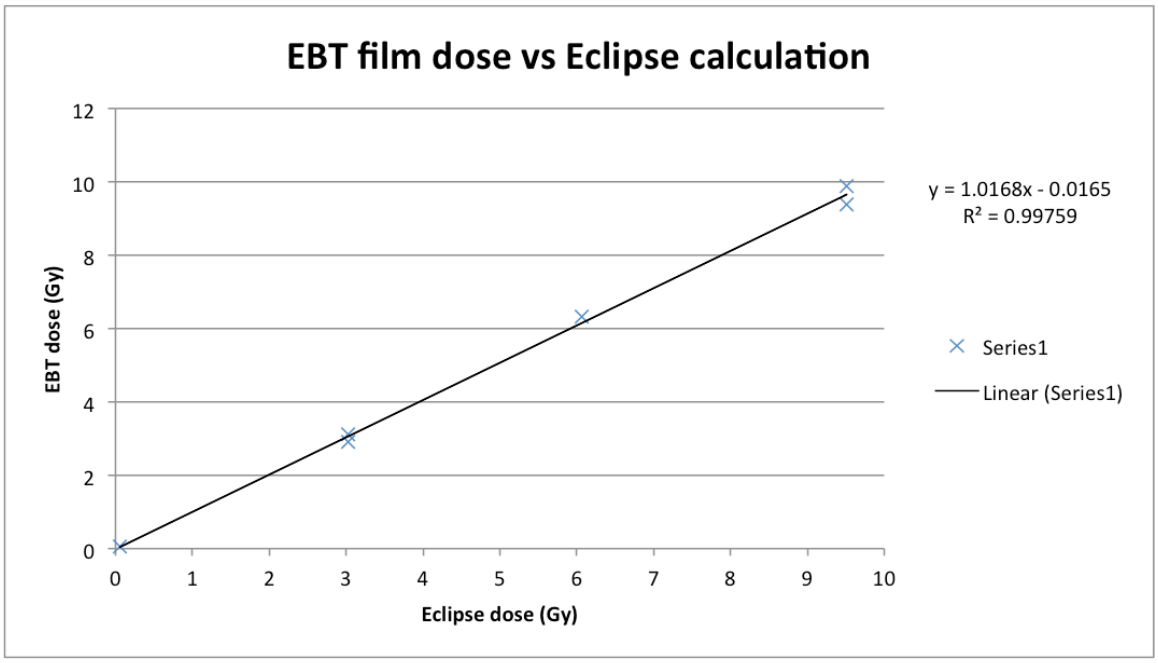

Figure 14: Plot comparing measured film dose and Eclipse dose calculation. Small variability of film dose is shown, however the regression exhibits excellent linearity ($R^2 = 0.998$).

3.5 Cuvette measurements

Because the temporal stability data showed that the DEA-1 formulation had the best absolute stability over the first few hours, and subsequently the best chance to be a viable large 3D dosimeter, the rest of the data will only be for that formulation.

3.5.1 DEA-1 cuvettes

The sensitivity of the cuvette measurements was measured to be 0.0289 OD/Gy/cm with an R^2 value of 0.99951. The intercept of the cuvette measurement was 0.0027 OD/Gy/cm

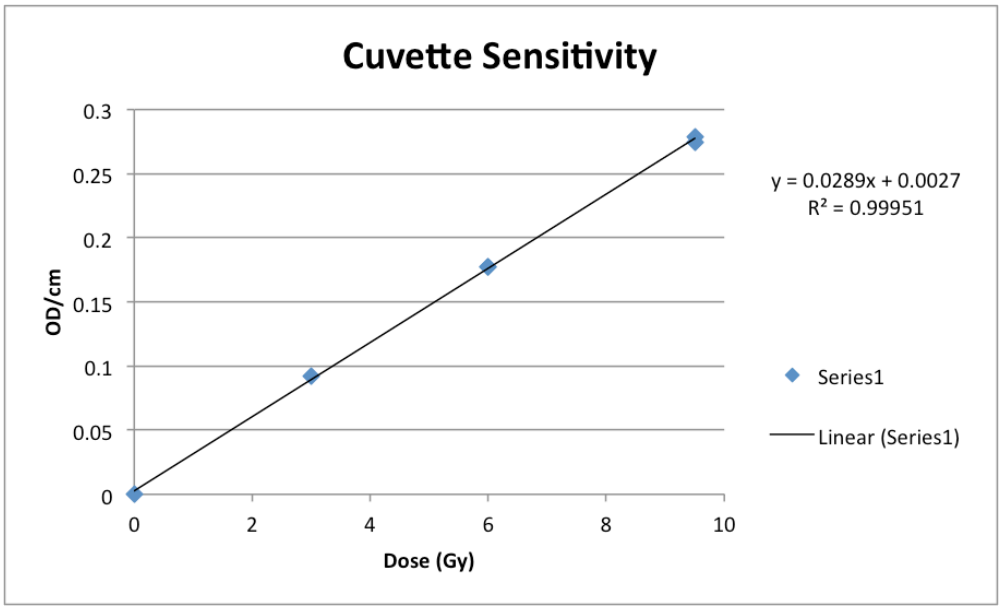

Figure 15: Sensitivity of DEA-1 cuvettes

3.5.2 Large dosimeter sensitivity vs. cuvette sensitivity

Since the idea of cuvettes is to use them for calibration to absolute dose in the large dosimeter, a comparison of the sensitivity of large dosimeter to cuvettes was done. The cuvettes and large dosimeter were irradiated to the same dose level of 3 Gy, 6 Gy, and 9.5 Gy (at a depth of d_{max} for the large dosimeter), a direct comparison of sensitivity can be made. Ideally, when the sensitivities of the cuvettes and large dosimeter are plotted against one another, the slope of the line should be 1 with an R^2 value of 1 and having an intercept of zero indicating that their sensitivities are equal for all dose levels. This was not the case for this formulation, however. The slope of the curve was 0.3694 indicating that the large dosimeter had less than half the sensitivity of the cuvettes. The linearity of the curve was very good with an R^2 value of 0.99934 and had an insignificant

intercept. It is important to note that the cuvettes were made from the same batch of Presage as the large dosimeter.

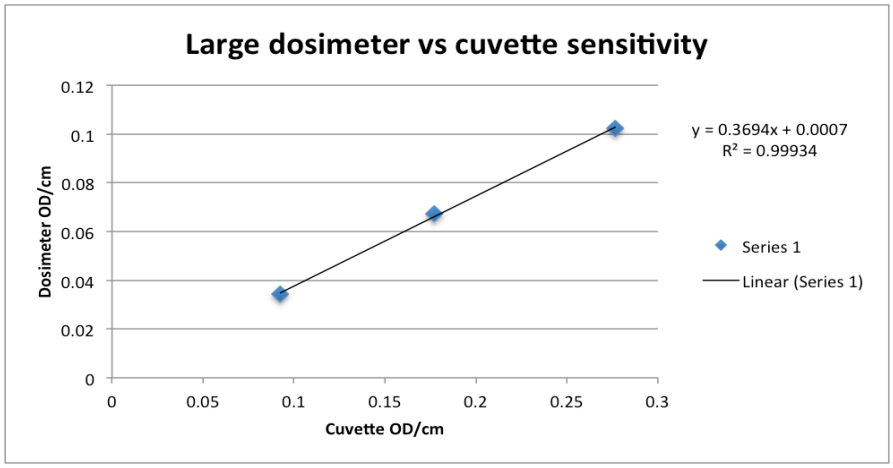

Figure 16: Sensitivity comparison of large dosimeter to cuvettes. Sensitivities of the dosimeter and cuvettes are compared at the same dose levels.

3.6 Presage and Delta^4 comparison

3.6.1 Relative Dosimetry comparison of Presage, Eclipse and Delta^4

In this section, Presage was used as a relative 3D dosimetry system, and later absolute dosimetry results will be discussed. For relative dosimetry, the optical density reading was scaled linearly to match the Eclipse dose distribution at one point in the high-dose region. The Presage and Eclipse dose distributions matched extremely well as evidenced by the next series of line profiles. The average dose difference between Presage and Eclipse in the high dose region was less than 2%. In the high gradient regions, Presage also did very well compared to Eclipse with less than 2 mm average distance to agreement. As shown by the dose profiles, the Delta^4 did not compare well to Eclipse. In the high dose regions, the average dose difference was generally less than

~3% although it reach as high as 6% difference. In the high gradient regions, line profiles routinely displayed distance to agreement of more than 3-4 mm.

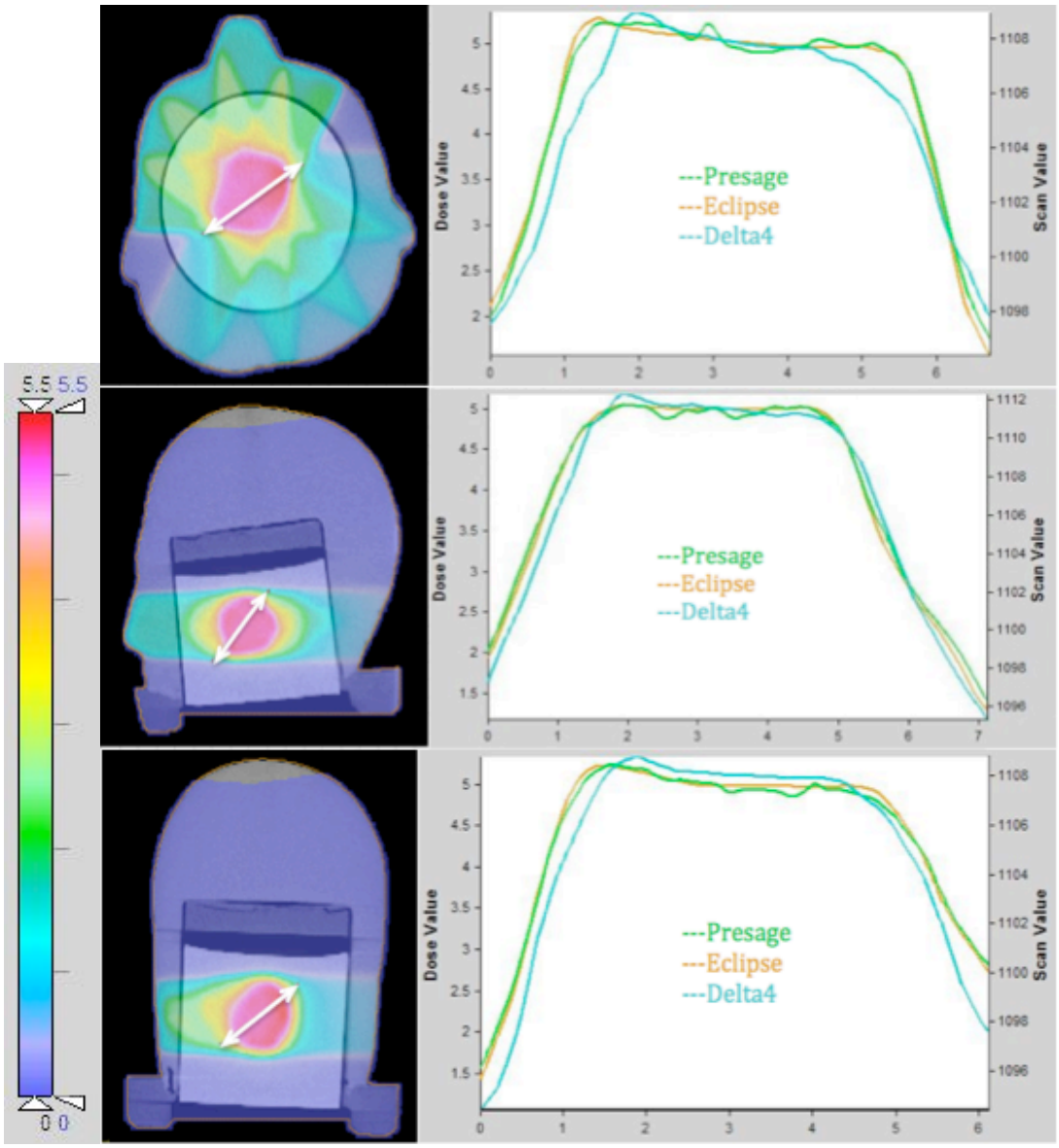

Figure 17: Line dose profiles through 3 viewing planes of the head and neck phantom. Axial (top), sagittal (middle), and coronal (bottom) slices. Presage distribution is relative dose.

3.6.2 3D Gamma Analysis

The criteria of 3%/3mm with a 10% threshold was used to compare the Delta^4 dose distribution to the relative Presage distribution and Eclipse. Some edge enhancing effects occurred in a ring of about 5 mm inside the edge of the dosimeter in the Presage distribution. This caused the apparent dose around the edge of the dosimeter to appear extremely high (~2x higher than actual dose). Because of this effect, the 3D gamma map was calculated after the edges of the dosimeter were cropped off to avoid those erroneously high values. The cause of this edge enhancing effect is not known and should be investigated further. The gamma maps below have been windowed so that any failing pixel (value > 1.0) appears red, and all other colors represent passing pixels. Presage displayed excellent agreement to Eclipse with a 3D gamma passing rate of 99.8%. Although the Delta^4 distribution mostly passes in the high-dose region, there are other large sporadic regions where the Delta^4 fails. The Delta^4 did not show exceptional agreement with a 3D gamma passing rate of 75.5%.

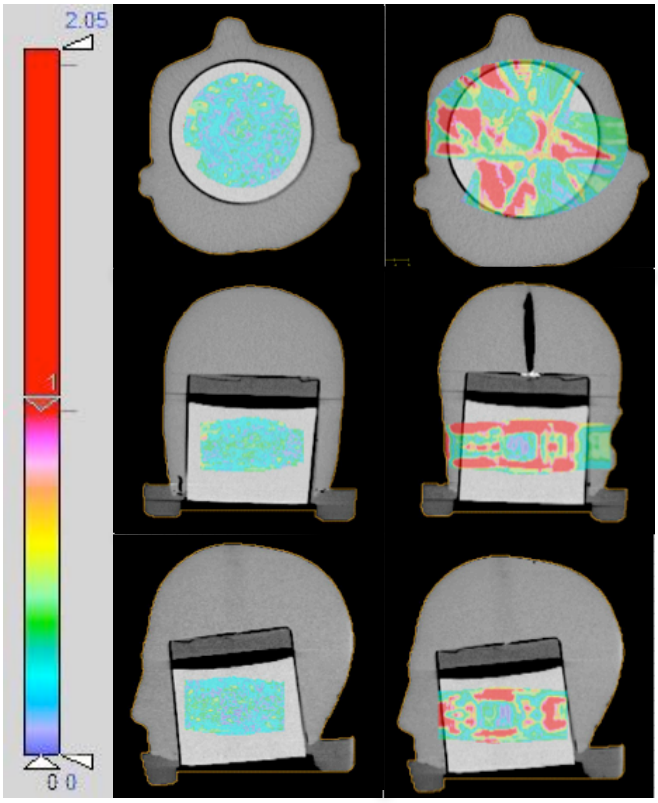

Figure 18: 3%/3mm gamma maps for Presage (left column) and the Delta^4 (right column) for axial (top), coronal (middle), and sagittal (bottom) planes. Both the Presage and Delta^4 distributions were compared with the Eclipse calculation. Red pixels are failing (>1), while all other colors represent passing pixels(<=1).

3.6.3 Absolute dose comparison

The absolute dose measured in the Presage phantom with the ion chamber was used to scale the optical density distribution measured with the optical-CT scanner. The absolute dose distribution was compared to Eclipse using line profiles and a 3D gamma analysis with a 3%/3mm criteria. The line profiles for absolute dose measurement of Presage match quite well with Eclipse, although the match is not quite as good as for the relative distribution. In the high dose region, the absolute Presage measurement was

generally about ~2% higher than the Eclipse prediction. In the gradient regions, the distributions matched quite well.

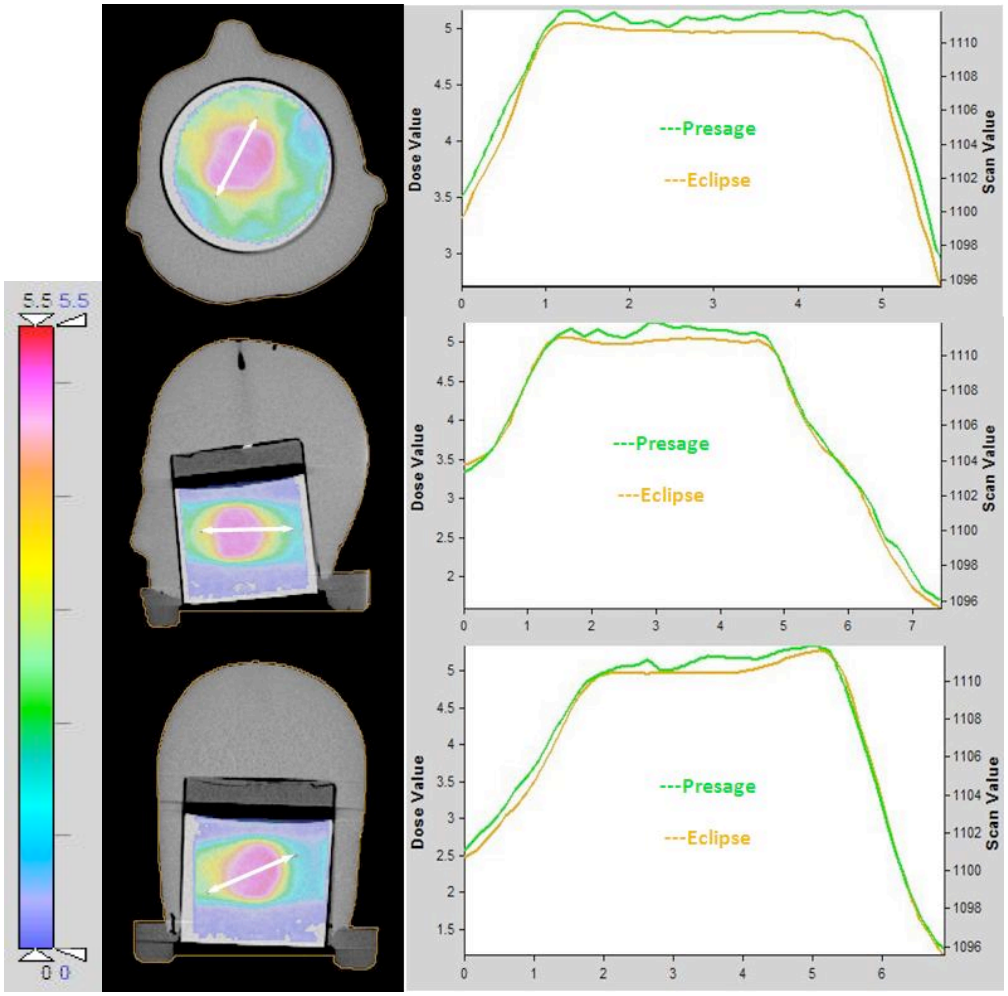

Figure 19: Line dose profile comparison of absolute Presage dose measurement with Eclipse calculation in axial (top), sagittal (middle), and coronal (bottom) planes.

The corresponding 3D gamma maps with 3%/3mm criteria are shown below. The passing rate for absolute Presage measurement was 99.6%. Although the line dose profiles through the Presage and Eclipse distributions did not agree as well as for the relative Presage distribution, the high gamma passing rate can be attributed to the fact that the gamma analysis was done in 3D dimensions providing an extra degree of freedom over 2D. All pixels shown as red are failing, while all others are passing.

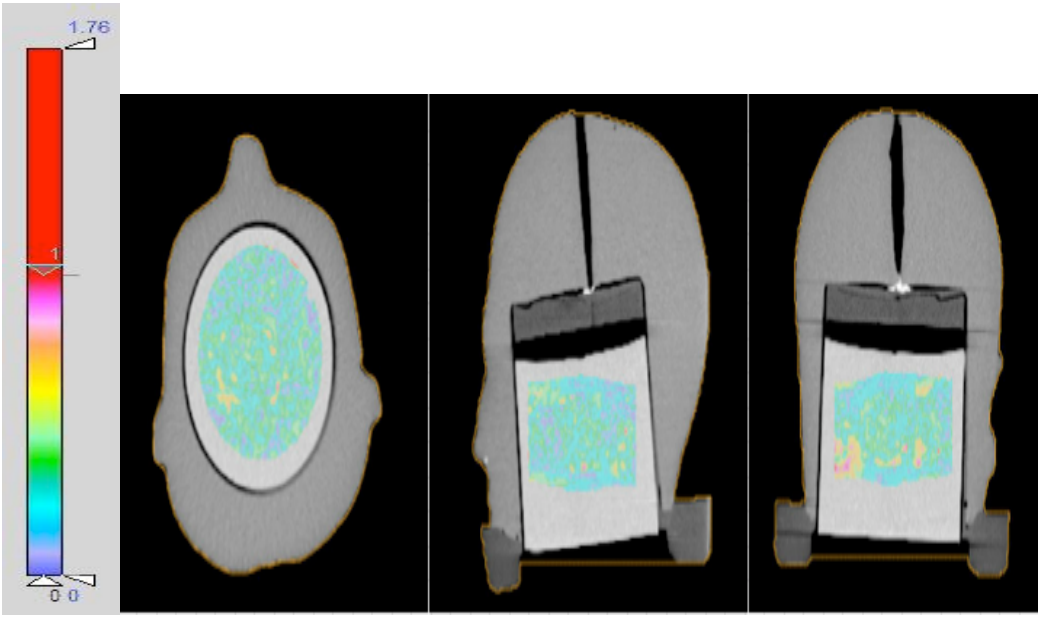

Figure 20: 3%/3mm gamma map between absolute Presage dose and Eclipse calculation for axial (left), sagittal (middle), and coronal (right) views. Red pixels (>1.0) are failing, and all other colors represent passing pixels.

4. Conclusions

One of the primary goals of this thesis was to characterize three new formulations of Presage in terms of temporal stability, sensitivity, linearity of dose response, and absolute calibration with cuvettes.

Of the three formulations, DEA-1 formulation had the best temporal stability through 24 hours post-irradiation, and for most accurate calibration to absolute dose, it is recommended that this formulation is scanned between 3 and 24 hours post-irradiation. The DEA-2 and DX formulations also show potential, although their temporal stability plots showed decreased sensitivity of up to ~10% and up to ~20%, respectively, through 24 hours. The DEA-2 formulation should be scanned between 2-6 hours post irradiation in order to ensure the most stable distribution. The DX formulation did not show temporal stability for any appreciable amount of time, however, the plot of sensitivity over time (figure 8) shows that the variation of sensitivity among the 5 beams was only $\pm 3.2\%$ at the 0-hour time point. Therefore, it is recommended that this formulation be scanned immediately post-irradiation. One area of concern for all formulations studied is the intercept, the point at which the sensitivity curve crosses the y-axis. This intercept should be very near zero, but a small, non-negligible, positive intercept was seen for all formulations. This could have significant implications for the relative dosimetry of Presage. If this effect is real, then it means simply scaling linearly from optical density to dose may not be valid in some

formulations, although the relative dosimetry approach worked well in the brain IMRT case. The cause of this intercept is not known, although a possibility is that the sensitivity is non-linear for small doses. A future direction of this work would be to study the sensitivity of these formulations to investigate the linearity of dose response at small doses (< 1 Gy).

As has been previously stated, absolute dosimetry is an important goal for Presage. One method for absolute calibration to dose is through irradiation of small volume cuvettes. The results of this experiment were not positive, and it seems absolute dosimetry using cuvettes isn't reliable yet, especially for large volume dosimeters. While some previous studies have shown cuvettes to come relatively close (~5-7%) to absolute dose, this work shows that the large dosimeters had a sensitivity less than half the sensitivity of cuvettes [19, 20]. This could be a formulation dependent measure, and there could be a volume effect causing the difference in sensitivity between cuvettes and large dosimeter. This effect is not understood and could provide a future direction of this work. An alternative to absolute calibration using cuvettes is to insert a small ion chamber into the Presage dosimeter and measure the dose to that point. The rest of the distribution can then be scaled linearly using the dose measurement at that point. This method has been shown to work well [17]. However, there could be some limitations such as noisy Presage data, which could lead to small (~1-2%) discrepancies.

The final goal of this work was to test the formulation with the best temporal stability and use the optimal imaging window determined from the studies above on a complex treatment. In this case, the DEA-1 formulation was irradiated with a brain IMRT case and was scanned 5 hours post-irradiation. The results of this study were phenomenal with 3D gamma passing rates (3%/3mm) for both the relative and absolute dose distributions exceeding 99%. Line dose profiles through the high dose regions showed that the relative dose distribution appeared to match the planned distribution better than the absolute dose, although the dose difference between the absolute distribution and planned distribution was acceptable (~2%). This 2% discrepancy can be attributed to a couple of factors. First of all, there could be some small error (1-2 mm) in the registration of the ion chamber within the Presage distribution. This could cause the wrong point in the Presage distribution to be scaled by the ion chamber reading. Some noise is also present in the Presage distribution (~1-2%), which could cause improper scaling of doses. The Delta^4 did not perform as well as expected with 3%/3mm gamma passing rate of 75.5%. This discrepancy could be attributed to the Delta^4 software's back-calculate of energy fluence from the diode measurements. In light of this study, strong evidence is shown for extremely accurate 3D dosimetry (~99%) when using optimal formulation and imaging procedures, and provides excellent validation of a complex IMRT treatment. Future work could compare Presage as a 3D quality assurance device with the Delta^4 or other 3D QA devices for additional complex treatments.

Additional figures

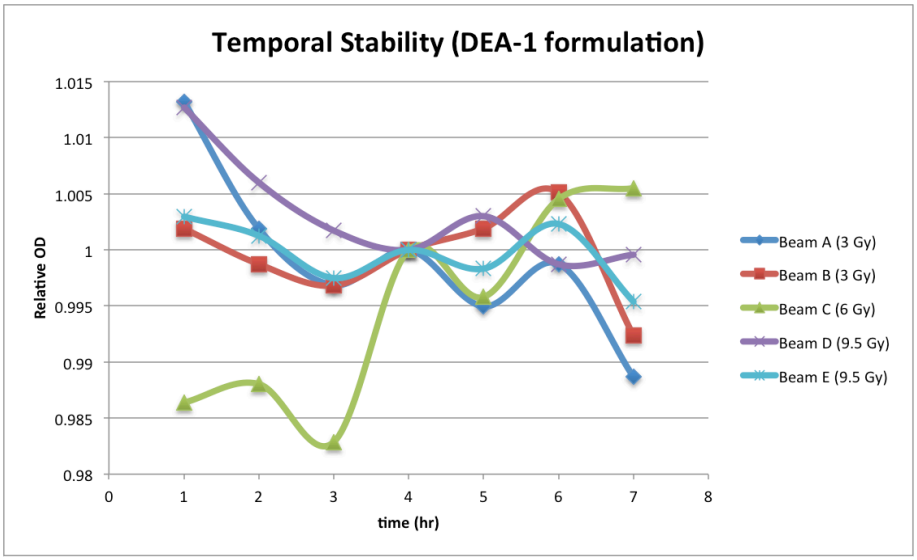

Figure 21: Repeated temporal stability measurement for different batch of DEA-1 formulation. Problems with the optical-CT scanner prevented scanning in the first hour post-irradiation.

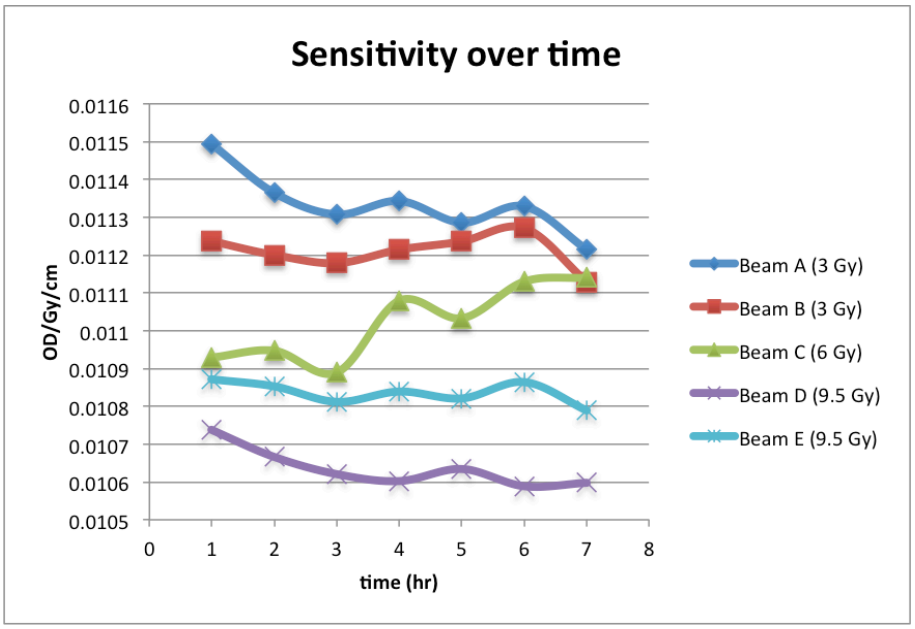

Figure 22: Sensitivity plot vs. time for same DEA-1 dosimeter as above temporal stability plot.

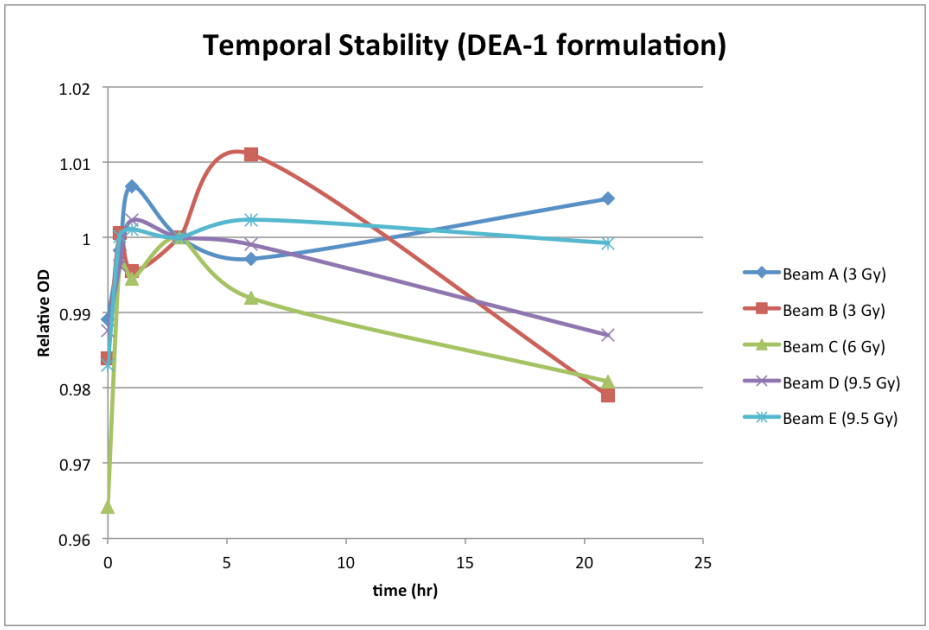

Figure 23: Repeated temporal stability measurement for different batch of DEA-1 formulation.

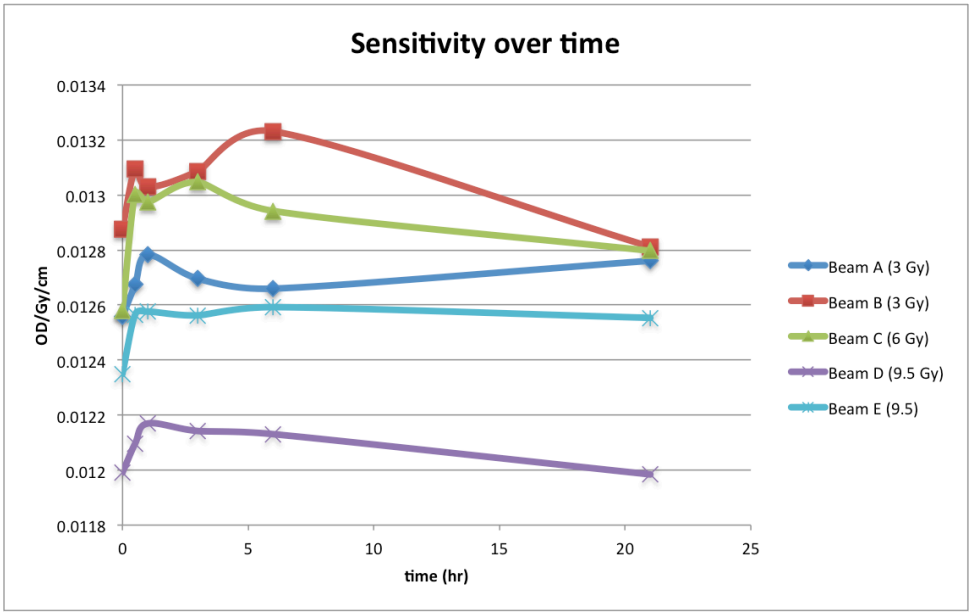

Figure 24: Sensitivity plot vs. time for same DEA-1 dosimeter as above temporal stability plot.

References

1. Molineu, Andrea, Nadia Hernandez, Trang Nguyen, Geoffrey Ibbott, and David Followill (2013). "Credentialing Results from IMRT Irradiations of an Anthropomorphic Head and Neck Phantom." *Medical Physics* 40(2)

2. LoSasso, T., C. S. Chui, et al. (2001). "Comprehensive quality assurance for the delivery of intensity modulated radiotherapy with a multileaf collimator used in the dynamic mode." *Medical Physics* 28(11): 2209-2219.

3. Wilcox, Ellen E., and George M. Daskalov (2007). "Evaluation of GAFCHROMIC® EBT Film for CyberKnife® Dosimetry." *Medical Physics* 34(6): 1967

4. Sukumar, Prabakar, Sriram Padmanaban, Prakash Jeevanandam, S.a. Syam Kumar, and Vivekanandan Nagarajan(2011). "A Study on Dosimetric Properties of Electronic Portal Imaging Device and Its Use as a Quality Assurance Tool in Volumetric Modulated Arc Therapy." *Reports of Practical Oncology & Radiotherapy* 16(6): 248-55

5. Van Esch, A., T. Depuydt, et al. (2004). "The use of an aSi-based EPID for routine absolute dosimetric pre-treatment verification of dynamic IMRT fields." *Radiotherapy and Oncology* 71(2): 223-234.

6. Li, Jonathan G., Guanghua Yan, Chihray Liu (2009). "Comparison of Two Commercial Detector Arrays for IMRT Quality Assurance." *Journal of Applied Clinical Medical Physics* 10(2)

7. Létourneau, Daniel, Misbah Gulam, Di Yan, Mark Oldham, and John W. Wong (2004). "Evaluation of a 2D Diode Array for IMRT Quality Assurance." *Radiotherapy and Oncology* 70(2): 199-206

8. Nelms, Benjamin E., Heming Zhen, and Wolfgang A. Tomé (2011). "Per-beam, Planar IMRT QA Passing Rates Do Not Predict Clinically Relevant Patient Dose Errors." *Medical Physics* 38(2)

9. Sadagopan, Ramaswamy, Jose A. Bencomo, Rafael Landrove Martin, Gorgen Nilsson, Thomas Matzen, and Peter A. Balter (2009). "Characterization and Clinical Evaluation of a Novel IMRT Quality Assurance System." *Journal of Applied Clinical Medical Physics* 10(2)

10. Feygelman, V., G. Zhang, et al. (2011). "Evaluation of a new VMAT QA device, or the "X" and "O" array geometries." *Journal of Applied Clinical Medical Physics* 12(2): 3346.

11. Baldock C, Harris P J, Piercy A R and Healy B (2001) “Experimental determination of the diffusion coefficient in 2D in ferrous sulphate gels using the finite element method” *Australas. Phys. Eng. Sci. Med.* 24: 19–30

12. Baldock, C., Y. De Deene, S. Doran, G. Ibbott, A. Jirasek, M. Lepage, K. B. Mcauley, M. Oldham, and L. J. Schreiner (2010). "Polymer Gel Dosimetry." *Physics in Medicine and Biology* 55(5)

13. Guo, P. Y., J. A. Adamovics, and M. Oldham (2006). "Characterization of a New Radiochromic Three-dimensional Dosimeter." *Medical Physics* 33(5)

14. Adamovics J, Maryanski MJ (2006). "Characterization of PRESAGE: A new 3-D radiochromic solid polymer dosimeter for ionizing radiation." *Radiation Protection Dosimetry* 120(1-4): 107-112

15. Sakhalkar HS, Adamovics J, Ibbott G, Oldham M, (2009) "A comprehensive evaluation of the PRESAGE/optical-CT 3D dosimetry system." *Medical Physics* 36: 71-82

16. Andrew Thomas, Michael Niebanck, Titania Juang, Zhiheng Wang and Mark Oldham (2013). "A comprehensive investigation of the accuracy and reproducibility of a multitarget single isocenter VMAT radiosurgery technique." *Medical Physics* 40(12)

17. Niebanck M (2012). "A Novel Comprehensive Verification Method for Multifocal RapidArc Radiosurgery Treatments." *Masters Thesis*, Duke University.

18. Mostaar A, Hashemi B, Zahmatkesh MH, Aghamiri SM, Mahdavi SR (2010) "A basic dosimetric study of PRESAGE: the effect of different amounts of fabricating components on the sensitivity and stability of the dosimeter." *Physics in Medicine and Biology* 55: 903-12

19. Sakhalkar H, Sterling D, Adamovics J, Ibbott G, Oldham M (2009) "Investigation of the feasibility of relative 3D dosimetry in the Radiological Physics Center Head and Neck IMRT phantom using Presage / optical CT." *Medical Physics* 36: 3371-77

20. Thomas, Andrew, Joseph Newton, John Adamovics, and Mark Oldham (2011). "Commissioning and Benchmarking a 3D Dosimetry System for Clinical Use." *Medical Physics* 38(8): 4846

21. Thomas, A., and M. Oldham (2010). "Fast, Large Field-of-view, Telecentric Optical-CT Scanning System for 3D Radiochromic Dosimetry." *Journal of Physics: Conference Series* 250: 012007

22. Adamovics, J., and M. J. Maryanski (2004). "A New Approach to Radiochromic Three-dimensional Dosimetry-polyurethane." *Journal of Physics: Conference Series* 3: 172-75

23. Guo P., Adamovics J., and Oldham M. (2006). "Practical three-dimensional dosimetry system for radiation therapy," *Medical Physics* 33: 3962–3972